Hindawi
Advances in Civil Engineering
Volume 2020, Article ID 8049626, 11 pages
https://doi.org/10.1155/2020/8049626

Research Article

Experimental Study and Damage Model Study of Rock Salt Subjected to Cyclic Loading and Cyclic Creep

Baoyun Zhao [1,2] Tianzhu Huang [2,3] Liu Dongyan, [2,3] Dongsheng Liu, [4] Yang Liu, [2,3] and Xiaoping Wang [2,3]

[1] *Graduate Office, Chongqing University of Science and Technology, Chongqing 401331, China*
[2] *Chongqing Key Laboratory of Energy Engineering Mechanics & Disaster Prevention and Mitigation, Chongqing 401331, China*
[3] *School of Civil Engineering and Architecture, Chongqing University of Science and Technology, Chongqing 401331, China*
[4] *Chongqing Bureau of Geology and Mineral Exploration, Chongqing 400391, China*

Correspondence should be addressed to Baoyun Zhao; baoyun666@163.com

Received 24 November 2019; Accepted 23 December 2019; Published 11 January 2020

Academic Editor: Paolo Castaldo

Due to the gas injection and production of underground salt caves during the operational phase, rock salt is often subjected to a combined stress of cyclic pressure and constant pressure. In order to investigate the damage evolution of rock salt under different combined stresses, the uniaxial cyclic loading test and cyclic creep test were carried out. The stress-strain curves, energy characteristics, energy dissipation, and damage of rock salt in the two experiments were analyzed and compared. The test results show that the stress-strain curves of the two tests presented three stages of "sparse"-"dense"-"sparse." As the maximum stress increases, the stage of "dense" will decrease and the rock salt cycle life will decrease. The relationship between cycle life and $\Delta\sigma$ (difference between maximum and minimum stress in the tests) is an exponential function under cyclic loading and a linear relationship under cyclic creep. Based on the experimental data, the energy dissipation of rock salt is analyzed. The damage variables were defined from the perspective of energy dissipation, and the damage evolution of rock salt under two tests was obtained. There are three corresponding stages of energy dissipation and damage: initial, constant speed, and acceleration. The damage model is obtained by inverse functioning the *s* function, and then the correction coefficient is added to the model to obtain the modified damage model. The modified damage model is compared with the experimental data. The results show that the model can accurately describe the three stages of rock salt damage. The significance of parameters in the modifying damage model is also discussed.

1. Introduction

Rock salt is considered as an ideal medium for underground storage of energy such as oil and natural gas due to its excellent characteristics of low porosity, low permeability, high-plastic deformation capacity, and self-repair capacity [1, 2]. In recent years, in the construction of underground energy storage in the rock salt and salt cavern-compressed gas energy storage power station in China, the construction and operation of the salt cavern in rock salt have been exerting cyclic loading on rock salt to varying degrees [3]. Therefore, it is of great significance to study the mechanical properties, energy characteristics, and damage evolution process of rock salt under cyclic loading for the long-term stability evaluation of salt cavern gas storage. Meanwhile, in practical engineering, the operation of rock salt gas storage mainly includes four stages: gas injection, constant high pressure, gas production, and constant low pressure, wherein gas injection and production are corresponding to cyclic loading and unloading procedures while the constant high and low pressure are similar to creep procedures. In order to ensure the long-term stability and safety of rock salt gas storage, it is necessary to study not only the fatigue characteristics but also the creep fatigue interaction of rock salt.

Currently, a lot of scholars have carried out in-depth research studies on deformation characteristics, fatigue properties, acoustic emission rules, and energy features of various rocks under cyclic loading [4–10]. Nejati and Ghazvinian [11] studied the fatigue damage evolution of three different brittle rock types (onyx marble, sandstone, and soft limestone). Yang et al. [12] applied cyclic loading on the coal samples and studied the strength, deformation, energy dissipation, and fatigue of the samples. Some scholars [13–15] have studied rock salt, indicating that fatigue characteristics are closely related to the stress, frequency, and velocity of loading. At the same time, some scholars [16, 17] have carried out cyclic creep loading tests of rock salt. Roberts et al. [18] carried out a triaxial cyclic loading creep test and a static creep test on rock salt to evaluate the cyclic effect of applied stress. Fan et al. [19] have shown that the cyclic life of rock salt in the cyclic creep test is significantly reduced within a certain range, and an empirical model of cycle life and interval time is established. In addition, many scholars [20–24] have studied the damage model of rocks under cyclic loading. However, the damage model for rock salt under cyclic creep loads is rarely studied. Therefore, it is very meaningful to propose a simple damage model of rock salt under cyclic loading and cyclic creep loading.

This paper analyzes the deformation characteristics and energy features of rock salt through the cyclic loading test and cyclic creep test under different maximum stress values. The damage variable is defined from the aspect of energy dissipation, the evolution law of rock salt damage in the two kinds of the cyclic test is found, and the modified damage model is established on the basis of inverse *S* function. The model can serve as a reference in the engineering design in the operating stage of rock salt gas storage.

2. Brief Introduction to Test

2.1. Sample Preparation. The rock salt samples were taken from the rock salt cores in the drilling process of oil and gas wells in Western China, and the core depth was about 800~1000 m. According to mineral content analysis, the main components are NaCl, Na_2SO_4, and insoluble substances and the proportion of rock salt is more than 80%. The insoluble substances are mainly calcium mirabilite mudstone, cloud limestone mudstone, and paste mudstone. The color of the samples is light yellow with an average natural density of 2.17 g/cm^3. The core is processed into a cylindrical solid standard sample with a height of 100 mm and a diameter of 50 mm (with a height to diameter ratio of 2 : 1) by using the indoor dry sawing method, as shown in Figure 1. The size of rock salt samples is required to be processed in strict accordance with the ISRM test procedures, with the allowable error range of 0.3 mm in diameter and the nonparallelism of upper and lower end faces of 0.05 mm. The wave velocity of the processed standard rock samples is measured, and the rock samples with similar wave velocity are selected for testing. The wave velocity of this batch of rock salt samples is about 3.030 km/s. The processed rock salt samples are numbered and wrapped with preservative films and stored in a dry sealed container.

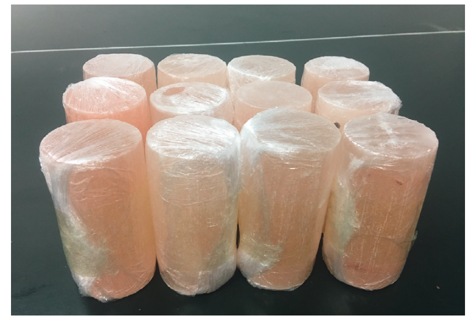

Figure 1: Rock salt samples.

Figure 2: YSSZ-500A Rock Biaxial Rheometer.

2.2. Test Equipment. A YSSZ-500A Rock Biaxial Rheometer is adopted in the test, as shown in Figure 2. As the main test equipment for the mechanical properties of materials such as rock and cement, the test equipment can be used in several tests, such as rock uniaxial, direct shear and rock shear creep, and fracturing tests by adopting advanced servo driving, sensor, microprocessor control, and handling technologies. The maximum axial compressive force of the test machine in the vertical direction is 500 kN, the maximum axial compressive force in the horizontal direction is 300 kN, and the pressure measurement error range is ±0.5%. During the test, the test data are automatically collected by microcomputers and recorded and analyzed in real time.

2.3. Test Method. In order to simulate the gas injection and gas production processes in the operation of the salt cavern, the two types of load paths are simulated by the cyclic loading and cyclic creep tests, as shown in Figure 3. The test adopts the load control method, and the loading and unloading speed is 2 kN/s. The maximum and minimum stresses are maintained for 1 hour in the cyclic creep test. The maximum and minimum stress values in the test are calculated by using the uniaxial peak strength, and the uniaxial peak strength $\sigma_c = 45.66$ MPa of rock salt is obtained by the uniaxial compression test with a loading speed of 0.5 MPa/s. Rock salt samples are difficult to obtain, so the same minimum stress and different maximum stress are used in the test, as shown in Table 1. During the test, the maximum stress that was too high caused the rock salt to break during the first loading. Finally, the test was only successful 7 times (excluding 3 times of the uniaxial compression test).

3. Analysis of Test Results and Energy Characteristics

3.1. Stress-Strain Curve. Figure 4 shows the stress-strain curve of rock salt under uniaxial cyclic loading and cyclic

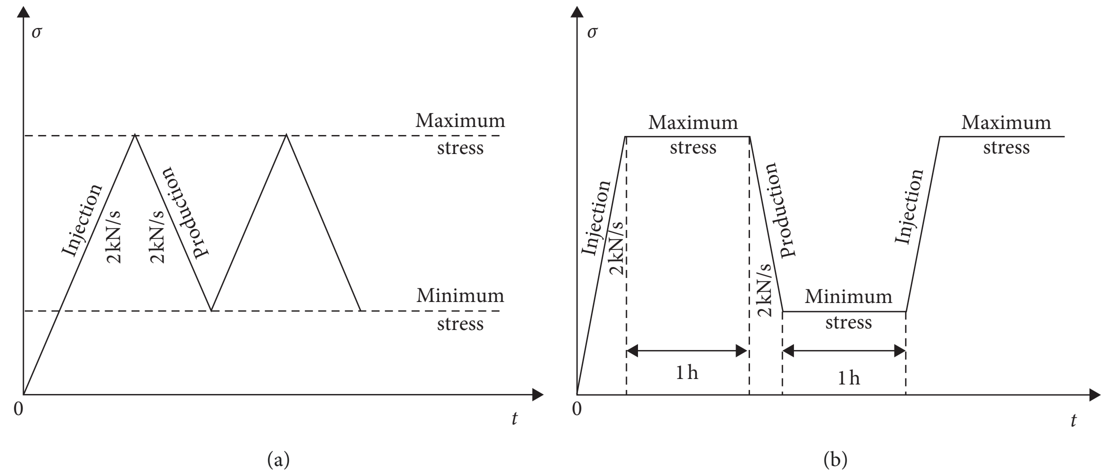

FIGURE 3: Path of loading and unloading for test. (a) Cyclic loading test and (b) cyclic creep test.

TABLE 1: Scheme for test of cyclic loading and cyclic creep.

Test type	No.	Maximum stress ratio (%)	σ_{max} (MPa)	Minimum stress ratio (%)	σ_{min} (MPa)	Holding time (h)
Cyclic loading	$X1$	70	31.96	20	9.13	0
	$X2$	75	34.25			
	$X3$	80	36.53			
	$X4$	85	38.81			
Cyclic creep	$R1$	60	27.40	20	9.13	1
	$R2$	65	29.68			
	$R3$	70	31.96			

Note: The maximum stress ratio in the table is the ratio between the maximum stress of the test load and the compressive strength of rock salt; the minimum stress ratio is the ratio between the minimum stress of the test load and the compressive strength of rock salt.

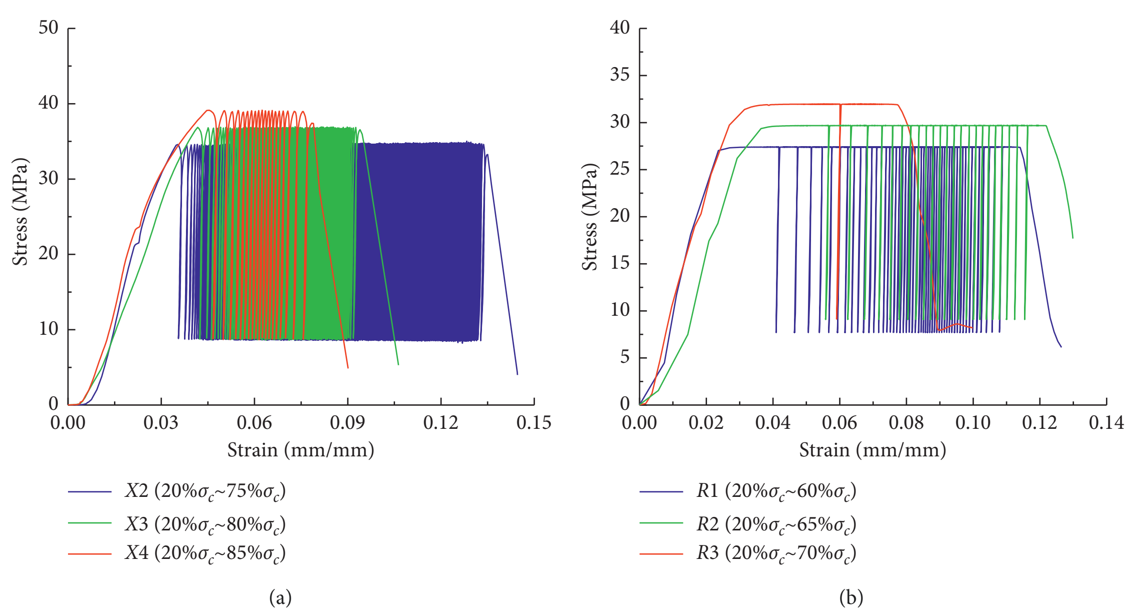

FIGURE 4: Stress-strain curve of rock salt. (a) Cyclic loading test and (b) cyclic creep test.

creep tests, and Table 2 shows the statistics of test results. From Figure 4, it can be seen that the two tests can both be divided into three stages. The first is the static loading stage, and the axial stress is loaded from 0 to the maximum stress value. The second is the cycle stage, where the axial stress is cyclically loaded and unloaded at the maximum and minimum stresses. The third is the damage stage which only exists in the process of sample failure. The stress-strain curve of rock salt basically shows three stages of "sparse," "dense," and "sparse," respectively, corresponding to the three stages

Table 2: Results of cyclic loading and cyclic creep tests on rock salt.

No.	Maximum stress value (MPa)	Minimum stress value (MPa)	Axial strain at damage point	Number of cycle (N)	Damage
$X1$	31.96	9.13	—	5422	Undamaged
$X2$	34.25		0.14	1591	Damaged
$X3$	36.53		0.09	154	Damaged
$X4$	38.81		0.08	19	Damaged
$R1$	27.40	9.13	0.11	51	Damaged
$R2$	29.68		0.12	23	Damaged
$R3$	31.96		0.08	1	Damaged

of the cyclic test [25]: the first stage is the initial stage, with large hysteretic curve spacing leading to a stress-strain curve showing the "sparse" state, resulting in a large plastic strain. The second stage is the stable stage, with more and more hysteresis loops, and the plastic strain produced by each cycle is relatively small. The third stage is the cycle acceleration stage, in which the hysteresis loop spacing and axial strain suddenly increase and the rock salt is damaged after several cycles. Meanwhile, it can be found that with the increase of the maximum stress value, the "dense" part of the stress-strain curve of rock salt will gradually decrease.

The cyclic life of the rock salt has a certain relationship with the maximum stress value. In the cyclic loading test, the rock salt was cycled 5422 times with a maximum stress of 70% σ_c without obvious damage. It can be considered that the damage effect caused by the maximum stress of 70% σ_c has very little influence on the mechanical properties of the rock salt sample, and it can be determined that the damage "threshold value" of the rock salt is from 70% σ_c to 75% σ_c. Meanwhile, it can be seen from Table 2 that the cycle life of rock salt decreases with the increase of maximum stress. The results of the two tests show that there is a significant relationship between $\Delta\sigma$ and the cycle life, where $\Delta\sigma$ is the maximum and minimum stress difference. The relationship between $\Delta\sigma$ and cycle life is an exponential function under cyclic loading and a linear relationship under cyclic creep (Figure 5).

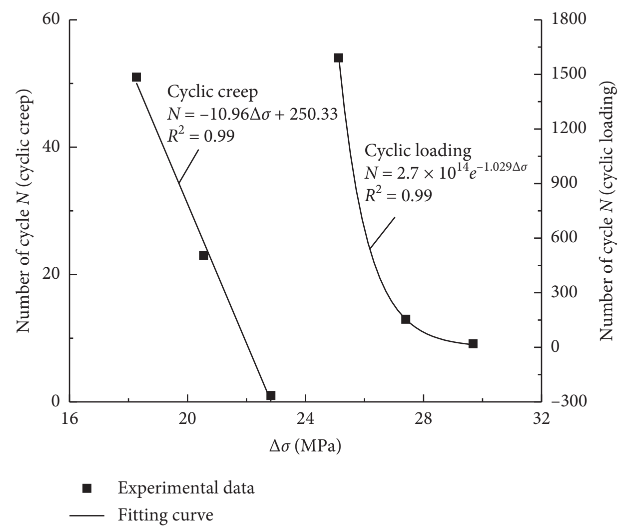

Figure 5: Cycle lifetime of rock salt under different loading conditions.

3.2. Energy Characteristics.

3.2. Energy Characteristics. For the loaded rock, the energy transformation process runs through the deformation: energy input, energy accumulation, energy dissipation, and energy release [26]. If it is assumed that there is no heat exchange between the rock sample and the outside in the process of deformation under load, the following conclusions can be derived from the first law of thermodynamics:

$$U = U^d + U^e, \tag{1}$$

where U is the total energy input to rock, U^d is the dissipate energy, and U^e is the releasable elastic strain energy.

Energy dissipation is the essential attribute in rock deformation and damage, which reflects the process of continuous closure of microdefects in rock, development and evolution of new fissures, constant weakening of material strength, and eventual loss [27]. Therefore, from the point of view of energy dissipation, the mechanical response characteristics of rock can be better explained. Part of the energy input to the rock from the outside forms reversible elastic strain energy which accumulates in the rock and can be released when unloaded. The other part dissipates in the form of acoustic energy, plastic deformation, and fissure propagation, which is called irreversible dissipative energy. During cyclic loading and unloading, some scholars [28] express dissipative energy by using the area of hysteresis loops (Figure 6). As can be seen from Figure 6

(1) The hysteresis loop curves of the cyclic loading test and cyclic creep test are often not closed and there is a certain residual strain. Therefore, the area S_1 of the hysteresis loop (BCD or ABCDE) cannot be used to represent the dissipated energy. In addition to the energy dissipated in the area S_1 of the hysteresis loop, the energy in the area S_3 is also dissipated [29].

(2) For the cyclic loading test, the BC section is the loading section, the stress-strain curve shows an upward trend, the pressure head of the test machine performs positive work on the rock salt, and the area below the BC curve is the total energy U input to the rock salt by the pressure head of the test machine, i.e., area $S_1 + S_2 + S_3$; the CD section is the unloading section, the stress and strain are decreasing, and the rock salt releases energy outward. The area integral below the BC curve is the elastic strain energy released by the rock salt U^e, which is the area S_2. From Equation (1), it can be seen that the total energy input

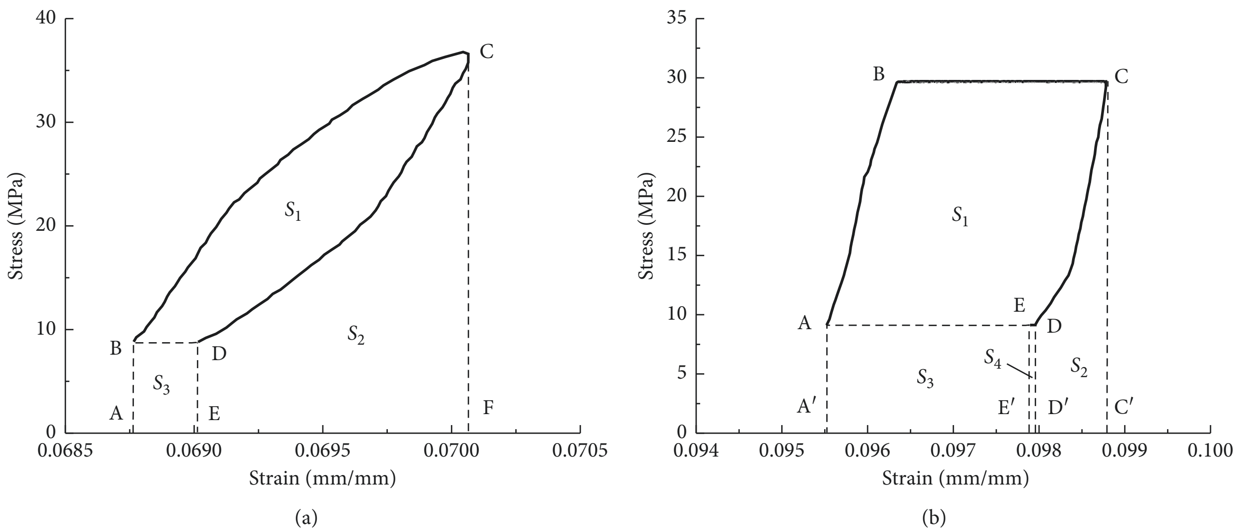

Figure 6: Typical hysteresis loop curve of rock salt. (a) The cycle number $n = 61$ of $X3$ rock salt in the cyclic loading test. (b) The cycle number $n = 15$ of $R2$ rock salt in the cyclic creep test.

to the rock from the outside minus the releasable elastic strain energy of the rock U^e is the energy dissipated by the rock U^d, that is, the area $S_1 + S_3$.

(3) For the cyclic creep test, section AB is the loading section, with increases both in stress and strain. Section BC is the holding section of the maximum stress value, and the stress remains unchanged while the strain is increasing all the time. The testing machine does positive work on the rock salt. Therefore, the area below the ABC curve is the total energy U input by the test machine, i.e., area $S_1 + S_2 + S_3 + S_4$. The CD section and DE section are the unloading section and the holding section of the minimum stress value, respectively. The area integral below the CDE curve is the elastic strain energy released by rock salt, i.e., $S_2 + S_4$. From the total energy U and the released elastic strain energy U^e, it can be concluded that the dissipation energy of rock salt U^d is the area $S_1 + S_3$.

(4) The total energy U in the cyclic loading test is mainly from the test machine, while in the cyclic creep test, more energy is inputted to the rock from the creep stage under the maximum stress value in addition to the loading stage; the rock salt will release the releasable elastic strain energy U^e in the unloading stage. In the cyclic creep test, in addition to the unloading stage, in the lower limit stress creep stage, the strain of the rock salt will be reduced and some elastic strain energy will be released at the same time. It can be seen from Figure 6(b) that the release of the elastic strain energy in the cyclic creep test is mostly completed in the unloading stage.

According to the different dissipation energy calculation methods mentioned above and in combination with the stress-strain curves of stress cyclic loading tests and cyclic creep tests, the variation of rock salt dissipation energy during the test is shown in Figure 7. Few points are mentioned as follows: ① in the cyclic loading test, the compaction stage of rock salt is included in the static loading stage. In the compaction stage, the dissipated energy is in several times to that of the cyclic stage. Such as 333.37 kJ·m^{-3} for the compaction stage of $X1$ sample and 41.98 kJ·m^{-3} for the first cycle. Therefore, for the convenience of analysis, only the relationship between the dissipation energy in the cyclic stage and the damage stage is analyzed. ② In the cyclic creep test, the $R3$ sample was damaged after only one complete cycle, so the change of its dissipation energy is not analyzed. ③ In the cyclic creep test, all rock salt damage occurs in the holding process of the maximum stress value in the creep stage. The stress-strain curve, when damage occurs, is not a complete hysteresis loop (as shown in Figure 4), but the energy dissipation generated at the previous loading stage and the creep stage of the maximum stress, when damage occurs, cannot be ignored. Therefore, the incomplete hysteresis loop, when damage occurs, shall be treated as a cycle when determining the influence of dissipation energy.

As can be seen from Figure 7, the curve is U-shaped and the U-shaped feature becomes more obvious with the increase of the maximum stress value. Therefore, the dissipation energy of the rock salt can be divided into three stages [30, 31]. In the initial stage, the dissipation energy of the rock salt drops sharply, mainly due to the existence of certain original microfissuring inside the rock salt and the closure of internal microdefects resulting in large macroscopic deformation and energy consumption, while the energy consumption gradually decreases as the rock salt is gradually compacted. In the constant speed stage, the dissipation energy tends to be stable. In this stage, the energy is mainly consumed in the production, effective expansion, and plastic deformation of microfissuring. The maximum stress value will affect the number of cycles in the constant speed stage. The higher the maximum stress value, the shorter the relative

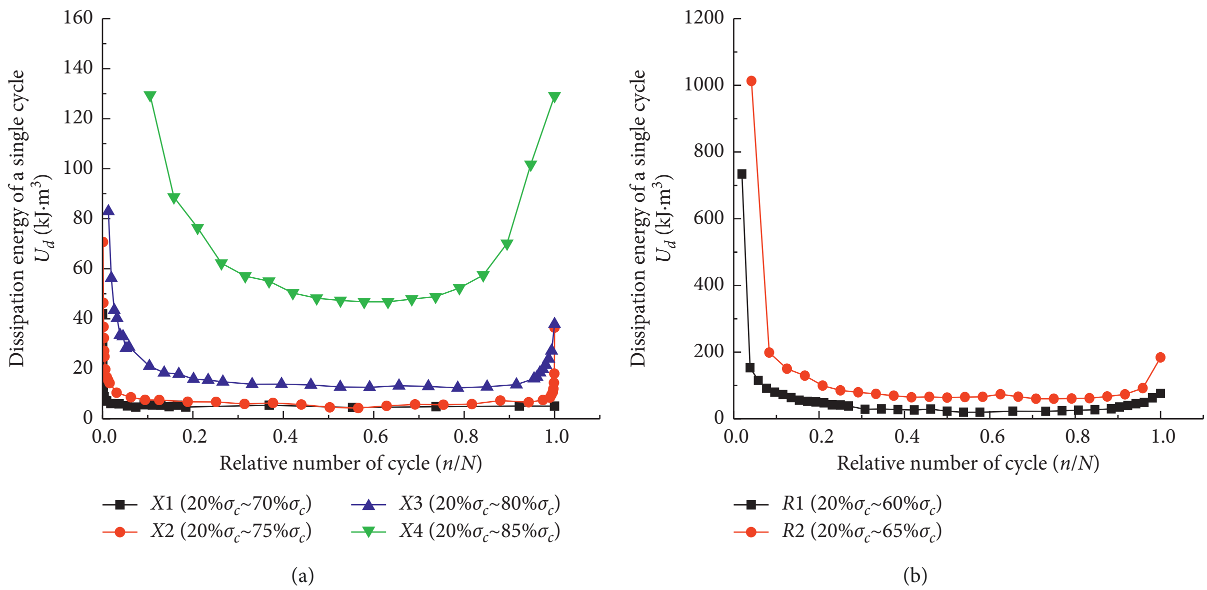

FIGURE 7: Dissipation energy of rock salt under different maximum stress. (a) Cyclic loading test and (b) cyclic creep test.

number of cycle in the constant speed stage. In the acceleration stage, the dissipation energy increases rapidly when the rock salt is about to be damaged, and the rock salt absorbs energy to make the internal microfissuring penetrate, showing macroscopic fissures. For rock salt with the maximum stress value below the fatigue "threshold value", there will be no acceleration stage, and the dissipation energy change curve will be L-shaped. Meanwhile, it can be seen that with the increase of the maximum stress value, the dissipation energy of the cycle will also increase, and the ratio of the number of cycle in the constant speed stage to all cycles will also decrease, thus accelerating the destruction speed of the rock salt.

4. Research of Rock Salt Damage Model

4.1. Damage Variable. The evolution process of damage variable can be considered as an irreversible evolution process of the internal structure of rock requiring energy consumption and can also reflect the deformation law of rock [32]: compaction of original microfissuring ⟶ production of new fissure ⟶ penetration of fissure ⟶ destruction. Usually, damage is studied from both macroscopic and microscopic perspectives, such as elastic modulus, stress, wave velocity, and the number of voids in the rock [33–35]. In addition, according to thermodynamics, energy dissipation is directly related to damage and strength loss. The amount of energy dissipation can reflect the degree of attenuation of the original strength. Meanwhile, both damage and energy dissipation are irreversible variables; therefore, they can define the internal damage of rock after reaching the maximum stress value and damages occur after a certain amount of energy dissipation. Then, the damage variable can be determined by using energy dissipation, and the expression is as follows:

$$D = \frac{\sum_{i=1}^{n} U_i^d}{\sum_{i=1}^{N} U_i^d}, \tag{2}$$

where $\sum_{i=1}^{n} U_i^d$ is the dissipated energy produced in the above n times cycles of rock salt and $\sum_{i=1}^{N} U_i^d$ is the sum of dissipated energy produced in all cycles of rock salt during rock salt damage.

The relation curve of damage variables of rock salt and the relative number of cycles under different maximum stress values is obtained by using data of cyclic loading tests and cyclic creep tests and damage variables calculated by Equation (2), as shown in Figure 8. The evolution process of rock salt damage shows three stages corresponding to energy dissipation. In the initial stage, the damage develops rapidly. The damage variable in the constant speed stage increased linearly. During the acceleration stage, the damage variable increases rapidly until the sample breaks. There is a certain connection between the three stages of damage development and the maximum stress value. The damage evolution curve becomes smooth as the maximum stress increases, indicating that the growth rate of the damage is similar in the three stages. Meanwhile, the damage caused by the cyclic creep test is significantly higher than the cyclic loading test at the initial stage. The damage evolution curve in the cyclic creep test is also smoother. The reason is that creep causes damage to rock salt, and creep causes more damage than fatigue damage in creep cyclic loading.

4.2. Establishment of the Model. When the maximum stress is high, the damage of rock salt shows three stages of deceleration, stability, and acceleration. For example, the damage evolution of $X4$ sample is shown in Curve 1 in Figure 9. If Curve 1 is symmetric with $D = n/N$ as the axis of symmetry, the inverse function of Curve 1 can be obtained,

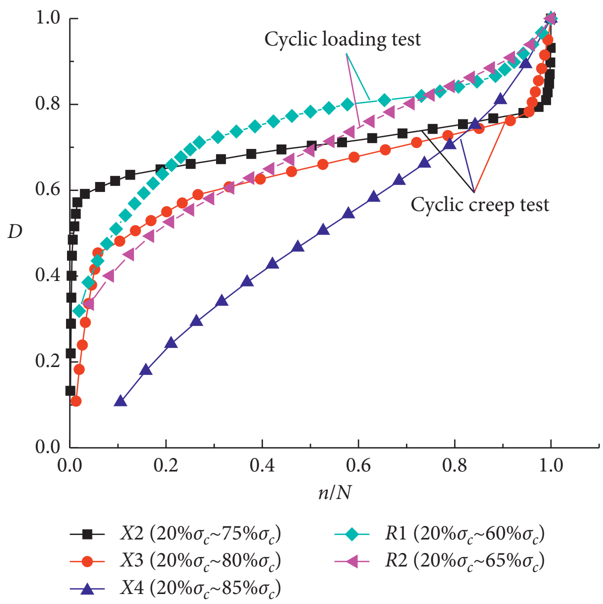

FIGURE 8: Evolution curve of damage variable under different maximum stress.

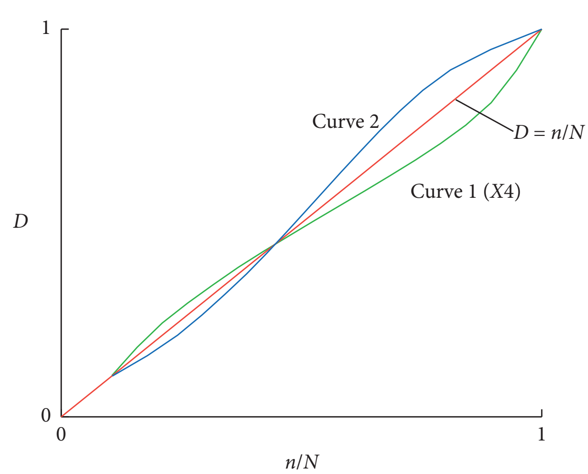

FIGURE 9: Rock salt damage evolution curve and inverse function.

that is, Curve 2 in Figure 9. Therefore, if the function expression of Curve 2 can be determined, the function expression of Curve 1, i.e., the equation of the damage variable evolution curve in the rock cycle test, can be determined by applying the properties of the inverse function.

As can be seen from Figure 9, Curve 2 as a whole is an S-shaped curve, so its expression can be shown by an S-shaped function. The functions commonly used to describe S-shaped curves are Logistic equation, Lo2logistic equation, Weibull equation, and Gompertz equation. Logistic function is one of the most widely used methods. Therefore, from the phenomenological point of view, the paper intends to establish damage models of rock salt by using the inverse function of logistic function.

The mathematical expression of logistic function is as follows:

$$y = \frac{c}{1 + e^{a-bx}}, \tag{3}$$

where x is the independent variable, y is the dependent variable, and a, b, and c are constants.

During the calculation of inverse function of Equation (3), the following can be obtained:

$$y = \frac{a}{b} - \frac{1}{b}\ln\left(\frac{c}{x} - 1\right). \tag{4}$$

When Equation (4) is applied to the damage model of rock salt in the above two kinds of cyclic tests, the independent variable x represents the relative number of cycles n/N and the dependent variable y represents the damage variable D of rock. Meanwhile, for the convenience of expression, $a/b = \alpha$ and $1/b = \beta$, then Equation (4) is as follows:

$$D = \alpha - \beta\ln\left(\frac{c}{n/N} - 1\right). \tag{5}$$

4.3. Damage Model Modification and Verification. Fitting the test results with the damage model of Equation (5), as shown in Figure 10, the model can describe the three processes of damage and the fitting effect is good when the maximum stress is high. However, when the maximum stress is low, the model does not work well for the first and third stages. This is because when the maximum stress is low, the damage of salt rock is mainly caused by rock compaction and crack development. Therefore, the damage rate in the first and third stages is much larger than that in the second stage and the slope of the curve changes greatly. The curve fitted by Equation (5) is relatively flat, and the three stages of damage are not accurately described. In order to make the change of the slope of the curve more obvious, Formula (5) is performed to the power of m. The modified model is as follows:

$$D = \left[\alpha - \beta\ln\left(\frac{c}{n/N} - 1\right)\right]^{m}, \tag{6}$$

where m is the correction factor.

The modified damage model of Equation (6) was fitted to the test results, as shown in Figure 10. The modified damage model is more accurate than the inverse s-curve model in describing the three stages of damage. The modified damage model can not only accurately reflect the changes of rock salt damage under cyclic loading but also under cyclic creep.

Values of parameters α, β, c, and m were obtained through fitting, as shown in Table 3. The parameters α, c, and m increase as the maximum stress increases. The parameter β increases with the increase of the maximum stress under the cyclic loading and decreases under the cyclic creep. It indicates that the parameter has a certain relationship with the maximum stress or the maximum and minimum stress difference. Some scholars have pointed out that the parameters of the damage model are related to the applied stress, loading rate, and frequency. This paper does not complete the cycle test under other different factors, so the equation between parameters and other factors cannot be obtained.

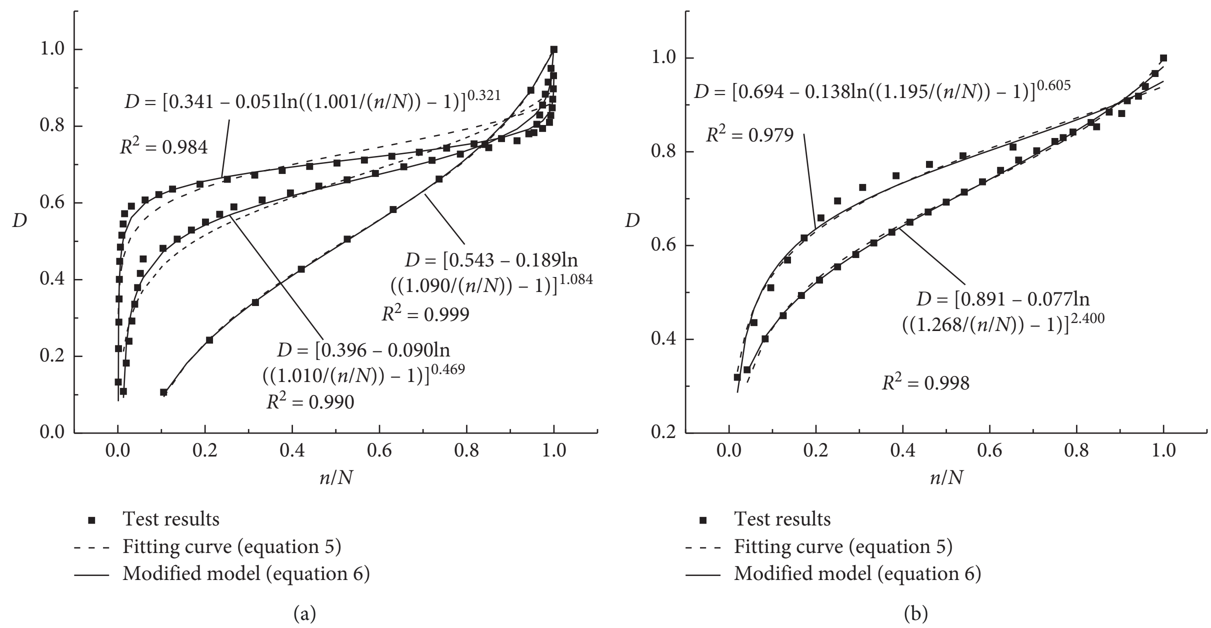

FIGURE 10: Damage variable fitting curve based on damage model. (a) Cyclic loading test and (b) cyclic creep test.

TABLE 3: Fitting results of parameters α, β, c, and m.

No.	Maximum stress ratio (%)	Parameter				R^2
		α	β	c	m	
$X2$	75	0.341	0.051	1.001	0.321	0.984
$X3$	80	0.396	0.090	1.010	0.469	0.990
$X4$	85	0.543	0.189	1.090	1.084	0.999
$R1$	60	0.694	0.138	1.195	0.605	0.979
$R2$	65	0.891	0.077	1.268	2.400	0.998

4.4. Significance of Model Parameters. In order to study the significance of parameters α, β, c, and m in Equation (6), a method of changing only one parameter and then observing the change of the image is employed, as shown in Figure 11. The significance of the parameter is obtained by analyzing the influence of the changed parameter on the damage model curve.

4.4.1. Significance of Parameter α. When β is 0.10, c is 1.05, m is 0.80, and α is 0.30, 0.35, 0.40, and 0.45, respectively. The parameter α will not affect the overall development trend of damage variables. But with the increase of α value, the damage value at the initial stage of damage will increase. Therefore, the parameter α controls the magnitude of the damage variable in the initial stage of the curve and can be defined as the speed factor of the damage in the initial stage.

4.4.2. Significance of Parameter β. When α is 0.40, c is 1.05, m is 0.80, and β is 0.05, 0.07, 0.09, and 0.11, respectively. The damage speed of the damage model curve with different parameters β is different at the constant speed stage. As the value of the parameter β increases, the slope of the damage model curve becomes larger at the constant speed stage. An increase in the slope indicates that the damage develops faster. Therefore, the value of the parameter β controls the growth rate of damage in the constant speed stage, which can be defined as the speed factor in the constant speed stage.

4.4.3. Significance of Parameter c. When α is 0.40, β is 0.10, m is 0.80, and c is 1.01, 1.04, 1.07, and 1.10, respectively. The curves of the initial stage and the constant speed stage of damage are approximately coincident. But the acceleration stage is obviously different, indicating that the parameter c has a certain correlation with the acceleration stage of the damage model curve. With the increase of the value of the parameter c, the curve in the acceleration phase becomes smoother, which also means the damage speed becomes slower and slower. Therefore, the parameter c controls the growth rate of damage in the acceleration stage, which can be defined as the speed factor in the acceleration stage. Meanwhile, it can be assumed that when the value of c is large enough, the damage growth rate approaches zero and the rock will not be damaged.

4.4.4. Significance of Parameter m. When α is 0.40, β is 0.10, c is 1.08, and m is 0.60, 0.80, 1.00, and 1.20, respectively. The parameter m has an effect on the whole process of the damage. As the parameter m increases, the damage model curve moves downward and the damage decreases. At the same time, it can be found that the change of m causes the change of the damage speed in the initial stage, the constant speed stage, and the acceleration stage. Therefore, the parameter m can be defined as the entire speed factor.

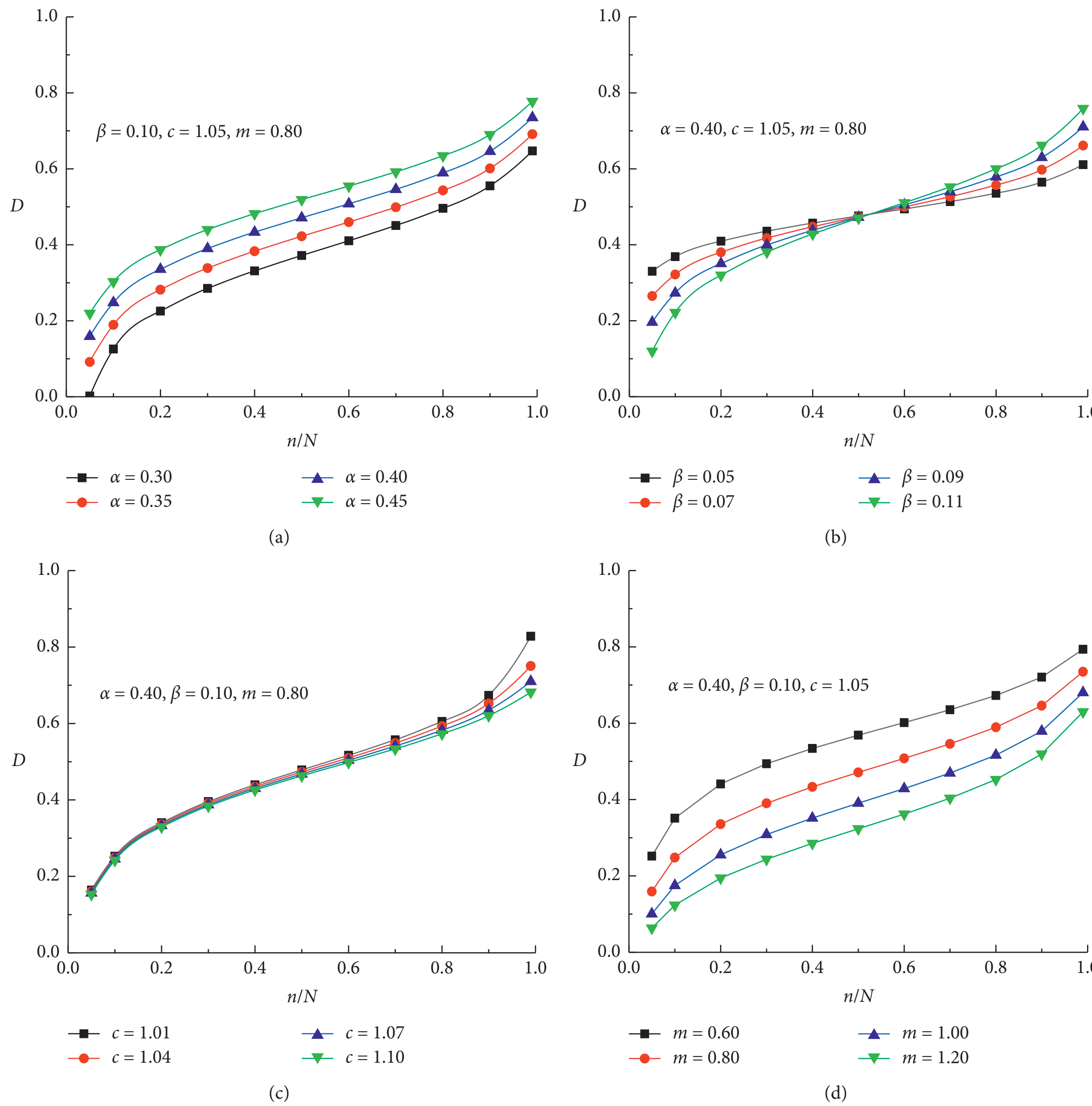

Figure 11: Influence of parameter (a) α, (b) β, (c) c, and (d) m on damage model curve.

5. Conclusion

Based on the cyclic loading test and cyclic creep test of rock salt under different maximum stress, the damage model of rock salt is established and the validity of the model is verified. The following conclusions can be drawn:

(1) In the cyclic loading test, the relationship between the rock salt cycle life and the maximum and minimum stress difference can be expressed by an exponential function. In the cyclic creep test, the cycle life is linear with the stress difference.

(2) The dissipative energy curves of rock salt under different maximum stress are U-shaped, which are mainly divided into initial stage, constant speed stage, and acceleration stage. Damage variables are determined by using the energy dissipation method, and the results show that the damage process of rock salt can also be divided into three stages corresponding to energy dissipation.

(3) The damage model is established based on the similarity between the damage evolution curve and the inverse function of the s-type function. By modifying the damage model, a modified damage model capable of accurately describing the three stages of damage evolution is obtained. Meanwhile, the significance of parameters α, β, c, and m in the model is analyzed as the damage speed factors in the initial stage, the constant speed stage, the acceleration stage, and the entire stage, respectively.

(4) The rationality of the modified damage model is verified by using test results of the uniaxial cyclic loading test and cyclic creep test of rock salt. The results show that the model can better describe the three stages of damage, especially the maximum stress is high. The model expression is very simple and the parameter meaning is clear, which is convenient to apply.

Data Availability

The data used to support the findings of this study are included within the article.

Conflicts of Interest

The authors declare that there are no conflicts of interest regarding the publication of this study.

Acknowledgments

The authors gratefully acknowledge the financial support from the Chongqing Research Program of Basic Research and Frontier Technology (cstc2016jcyjA0302) and Scientific and Technological Research Program of Chongqing Municipal Education Commission (KJ1713324).

References

[1] H. P. Xie, J. F. Liu, Y. Ju, J. Li, and L. Z. Xie, "Fractal property of spatial distribution of acoustic emissions during the failure process of bedded rock salt," *International Journal of Rock Mechanics and Mining Sciences*, vol. 48, no. 8, pp. 1344–1351, 2011.

[2] P. Li, J. C. Deng, W. L. Zhao, and Y. C. Feng, "An experimental study on creep characteristics of salt rock and gypsum-salt rock in puguang gas field," *Petroleum Science and Technology*, vol. 30, no. 16, pp. 1715–1724, 2012.

[3] Y. T. Guo, K. L Zhao, G. Shun et al., "Experimental study of fatigue deformation and damage characteristics of rock salt under cyclic loading," *Rock and Soil Mechanics*, vol. 32, no. 5, pp. 1353–1359, 2011.

[4] S. K. Ray, M. Sarkar, and T. N. Singh, "Effect of cyclic loading and strain rate on the mechanical behaviour of sandstone," *International Journal of Rock Mechanics and Mining Sciences*, vol. 36, no. 4, pp. 543–549, 1999.

[5] Y. J. Yang, H. Q. Duan, L. Y. Xing, S. Ning, and J. K. Lv, "Fatigue characteristics of limestone under triaxial compression with cyclic loading," *Advances in Civil Engineering*, vol. 2018, Article ID 8681529, 12 pages, 2018.

[6] J.-Q. Xiao, D.-X. Ding, F.-L. Jiang, and G. Xu, "Fatigue damage variable and evolution of rock subjected to cyclic loading," *International Journal of Rock Mechanics and Mining Sciences*, vol. 47, no. 3, pp. 461–468, 2010.

[7] A. Araei Aghaei, H. R. Razeghi, A. Ghalandarzadeh, and S. Hashemi Tabatabaei, "Effects of loading rate and initial stress state on stress-strain behavior of rock fill materials under monotonic and cyclic loading conditions," *Scientia Iranica*, vol. 19, no. 5, pp. 1220–1235, 2012.

[8] H. Duan and Y. Yang, "Deformation and dissipated energy of sandstone under uniaxial cyclic loading," *Geotechnical and Geological Engineering*, vol. 36, no. 1, pp. 611–619, 2018.

[9] S.-Q. Yang, W.-L. Tian, and P. G. Ranjith, "Experimental investigation on deformation failure characteristics of crystalline marble under triaxial cyclic loading," *Rock Mechanics and Rock Engineering*, vol. 50, no. 11, pp. 2871–2889, 2017.

[10] Q. Meng, M. Zhang, L. Han, H. Pu, and Y. L. Chen, "Acoustic emission characteristics of red sandstone specimens under uniaxial cyclic loading and unloading compression," *Rock Mechanics and Rock Engineering*, vol. 51, no. 4, pp. 969–988, 2018.

[11] H. R. Nejati and A. Ghazvinian, "Brittleness effect on rock fatigue damage evolution," *Rock Mechanics and Rock Engineering*, vol. 47, no. 5, pp. 1839–1848, 2014.

[12] Y. J. Yang, L. Y. Xing, H. Q. Duan, L. Deng, and Y. C. Xue, "Fatigue damage evolution of coal under cyclic loading," *Arabian Journal of Geosciences*, vol. 11, no. 18, p. 560, 2018.

[13] S. Ren, Y. M. Bai, J. P. Zhang, D. Y. Jiang, and C. H. Yang, "Experimental investigation of the fatigue properties of salt rock," *International Journal of Rock Mechanics and Mining Sciences*, vol. 64, pp. 68–72, 2013.

[14] L.-J. Ma, X.-Y. Liu, M.-Y. Wang et al., "Experimental investigation of the mechanical properties of rock salt under triaxial cyclic loading," *International Journal of Rock Mechanics and Mining Sciences*, vol. 62, pp. 34–41, 2013.

[15] C. Wang, J. Liu, and L. Wang, "Damage evolution characteristics of rock salt under different stress conditions," *Advances in Civil Engineering*, vol. 2019, Article ID 3073975, 12 pages, 2019.

[16] D. Jiang, J. Fan, J. Chen, L. Li, and Y. Cui, "A mechanism of fatigue in salt under discontinuous cycle loading," *International Journal of Rock Mechanics and Mining Sciences*, vol. 86, pp. 255–260, 2016.

[17] J. Fan, D. Jiang, W. Liu, F. Wu, J. Chen, and J. Daemen, "Discontinuous fatigue of salt rock with low-stress intervals," *International Journal of Rock Mechanics and Mining Sciences*, vol. 115, pp. 77–86, 2019.

[18] L. A. Roberts, S. A. Buchholz, K. D. Mellegard, and U. Düsterloh, "Cyclic loading effects on the creep and dilation of salt rock," *Rock Mechanics and Rock Engineering*, vol. 48, no. 6, pp. 2581–2590, 2015.

[19] J. Fan, J. Chen, D. Jiang, S. Ren, and J. Wu, "Fatigue properties of rock salt subjected to interval cyclic pressure," *International Journal of Fatigue*, vol. 90, pp. 109–115, 2016.

[20] N. Li, W. Chen, P. Zhang, and G. Swoboda, "The mechanical properties and a fatigue-damage model for jointed rock masses subjected to dynamic cyclical loading," *International Journal of Rock Mechanics and Mining Sciences*, vol. 38, no. 7, pp. 1071–1079, 2001.

[21] M. He, N. Li, C. Zhu, Y. Chen, and H. Wu, "Experimental investigation and damage modeling of salt rock subjected to fatigue loading," *International Journal of Rock Mechanics and Mining Sciences*, vol. 114, pp. 17–23, 2019.

[22] J.-Q. Xiao, X.-T. Feng, D.-X. Ding, and F.-L. Jiang, "Investigation and modeling on fatigue damage evolution of rock as a function of logarithmic cycle," *International Journal for Numerical and Analytical Methods in Geomechanics*, vol. 35, no. 10, pp. 1127–1140, 2011.

[23] B. Sun, Z. Zhu, C. Shi, and Z. Luo, "Dynamic mechanical behavior and fatigue damage evolution of sandstone under cyclic loading," *International Journal of Rock Mechanics and Mining Sciences*, vol. 94, pp. 82–89, 2017.

[24] H. Haghgouei, A. Baghbanan, and H. Hashemolhosseini, "Fatigue life prediction of rocks based on a new bi-linear damage model," *International Journal of Rock Mechanics and Mining Sciences*, vol. 106, pp. 20–29, 2018.

[25] J. Liu, H. Xie, Z. Hou, C. Yang, and L. Chen, "Damage evolution of rock salt under cyclic loading in unixial tests," *Acta Geotechnica*, vol. 9, no. 1, pp. 153–160, 2013.

[26] Z. Chen, C. He, D. Wu, G. Xu, and W. Yang, "Fracture evolution and energy mechanism of deep-buried carbonaceous slate," *Acta Geotechnica*, vol. 12, no. 6, pp. 1243–1260, 2017.

[27] M. He, B. Huang, C. Zhu, Y. Chen, and N. Li, "Energy dissipation-based method for fatigue life prediction of rock salt," *Rock Mechanics and Rock Engineering*, vol. 51, no. 5, pp. 1447–1455, 2018.

[28] M. N. Bagde and V. Petroš, "Fatigue and dynamic energy behaviour of rock subjected to cyclical loading," *International Journal of Rock Mechanics and Mining Sciences*, vol. 46, no. 1, pp. 200–209, 2009.

[29] Y. Liu, F. Dai, L. Dong, N. Xu, and P. Feng, "Experimental investigation on the fatigue mechanical properties of intermittently jointed rock models under cyclic uniaxial compression with different loading parameters," *Rock Mechanics and Rock Engineering*, vol. 51, no. 1, pp. 47–68, 2018.

[30] R. Peng, Y. Ju, J. G. Wang, H. Xie, F. Gao, and L. Mao, "Energy dissipation and release during coal failure under conventional triaxial compression," *Rock Mechanics and Rock Engineering*, vol. 48, no. 2, pp. 509–526, 2015.

[31] E. B. Li, L. Gao, X. Q. Jiang et al., "Analysis of dynamic compression property and energy dissipation of salt rock under three-dimensional pressure," *Environmental Earth Sciences*, vol. 78, p. 388, 2019.

[32] S.-L. Qiu, X.-T. Feng, J.-Q. Xiao, and C.-Q. Zhang, "An experimental study on the pre-peak unloading damage evolution of marble," *Rock Mechanics and Rock Engineering*, vol. 47, no. 2, pp. 401–419, 2013.

[33] A. Schubnel, P. M. Benson, B. D. Thompson, J. F. Hazzard, and R. P. Young, "Quantifying damage, saturation and anisotropy in cracked rocks by inverting elastic wave velocities," *Pure and Applied Geophysics*, vol. 163, no. 5-6, pp. 947–973, 2006.

[34] S.-E. Lee, M.-I. Kim, J.-H. Park, C.-K. Park, M. Kang, and G.-C. Jeong, "Damage process of intact granite under uniaxial compression: microscopic observations and contact stress analysis of grains," *Geosciences Journal*, vol. 10, no. 4, pp. 457–463, 2006.

[35] Y. Wang, Z. Q. Hou, and Y. Z. Hu, "In situ X-ray micro-CT for investigation of damage evolution in black shale under uniaxial compression," *Environmental Earth Sciences*, vol. 77, p. 717, 2018.


Journal of Engineering
The Scientific World Journal
International Journal of Rotating Machinery
Journal of Sensors
Advances in Multimedia
Advances in Civil Engineering
Hindawi
Submit your manuscripts at
www.hindawi.com
Journal of Control Science and Engineering
Journal of Robotics
Journal of Electrical and Computer Engineering
Advances in OptoElectronics
VLSI Design
International Journal of Navigation and Observation
Modelling & Simulation in Engineering
International Journal of Aerospace Engineering
International Journal of Chemical Engineering
International Journal of Antennas and Propagation
Active and Passive Electronic Components
Shock and Vibration
Advances in Acoustics and Vibration